Indian J. Phys. **73B** (4), 593-604 (1999)

IJP B
— an international journal

Current driven oblique whistler wave in the magnetosphere of Uranus

R P Pandey, K K Singh, K M Singh and R S Pandey*
Department of Physics, Veer Kunwar Singh University, Ara-802 301, Bihar, India

Received 24 September 1998, accepted 30 March 1999

Abstract : Strong electromagnetic and electrostatic plasma turbulence, low frequency radio emissions and dust impacts were readily detected during the Voyager 2 encounter of Uranus. Examination of magnetic field data recorded in closed proximity to the Uranian bow shock reveals a series of whistler wave events. Some of the waves exhibited propagation parallel to the magnetic field but most showed oblique propagation. a.c electric field observations at magnetospheric heights and shock regions have also been reported along and perpendicular to the magnetic field In the present paper, oblique whistler mode instabilities have been analyzed having [$k_{\parallel}$ & $k_{\perp}$] wave numbers for a generalized drifted distribution function, reducible to bi-Maxwellian and loss-cone distribution in the presence of perpendicular a.c. electric field by method of characteristic solution Using details of particle trajectories, dispersion relation and growth rate have been evaluated. Results have been discussed and applied to the magnetosphere of Uranus.

Keywords : Oblique whistler, wave, mode instabilities, magnetosphere of Uranus.

PACS Nos. : 52.35. Qz. 94.30. Gm

1. Introduction

In the initial summary reports on the Voyager 2 plasma wave observations at Uranus, Gurnett and coworkers [1-3] demonstrated that strong electromagnetic and electrostatic plasma turbulence, low frequency radio emissions and dust impacts were readily detected during the encounter. Whistler emissions begin near spacecraft event time [SCET] 1500 at frequency $f = 560$ Hz, increase in frequency as the electron cyclotron frequency f_{c_e} rises towards closest approach and reach maximum intensity in the frequency band 311 Hz $< f <$ 1 kHz. The most intense whistler signals have been observed in the 562-Hz channel, which corresponds to a normalized frequency $\overline{\omega} = f/f_{c_e}$ in the range $\overline{\omega} = 0.22$ [SCET 2000] to $\overline{\omega} = 0.35$ [SCET 2030]. Whistler emissions in this normalized frequency range are commonly observed on auroral L

* Department of Applied Physics, I.T., Banaras Hindu University, Varanasi-221 005, Uttar Pradesh, India.

shells in both the terrestrial and Jovian magnetospheres. The Uranian whistler emissions fluctuate from measurement to measurement by factors of 3 to greater than 10 [4].

A preliminary analysis of Voyager 2 observations [5] revealed an intrinsic planetary magnetic field of Uranus. Lower frequency whistler waves have been reported at Saturn [6] and Uranus [7,8]. The encounter of Voyager 2 spacecraft with the uranian planetary system led to a series of outbound crossing of the Uranian bow shock between January 27 and January 30 of 1986. Examination of magnetic field data recorded in closed proximity to the shock, reveals a series of Whistler wave events that appear to result from processes associated with the shock. Some of the waves exhibited propagation parallel to the magnetic field but most showed oblique propagation. A.C. electric field observations at magnetospheric heights and shock region have also been reported along and perpendicular to the magnetic field [9-11].

Parallel propagating Plasma waves in the vicinity of the magnetopause at ELF/VLF frequencies have been studied by many workers [12-19], whistler mode instabilities were analyzed using data from magnetosphere and electron experiment on board ISEE and AMPTE-UKS [20-22]. The growth of whistler wave was also investigated from an anisotropic electron beam of various electrostatic and electromagnetic wave modes at various propagation angles using a series of 1-d simulations [23]. However, wave propagation was still restricted to a single fixed direction relative to the magnetic field. Devine *et al* [24] generalized oblique whistler mode instability in one and two dimensional simulations.

Electron beam excitation of upstream waves in the whistler mode frequency range was also studied in interplanetary space at 1 A.U. Both parallel and obliquely propagating solutions were considered [25]. Whistler waves have been observed in upstream from obliquely propagating shock waves in both simulations and space plasma [26, 27]. For a solar wind type plasma, expected wavelength are of the order of inertial length and depend on obliquely propagating speed and field orientation [28, 29].

Recently, competing processes of anisotropic electron beam having linear results and two dimensional particle simulations [30] of oblique whistler mode instabilities with relevance to interpretation of wave activities observed in Earth's magnetosphere by the GEOS 1, GEOS 2 and GEOTAIL satellites or in Uranian bow shock by Voyager 2 were proposed.

In the present paper therefore, oblique whistler mode instabilities have been analyzed having [$k_\perp$ and $k_\parallel$] wave numbers for a generalized drifted distribution function, reducible to bi-Maxwellian and Loss-Cone distribution in the presence of perpendicular a.c. electric field by method of characteristic solutions. Using the details of particle trajectories [19], dispersion relation and growth rate have been evaluated. Results have been discussed and applied to the magnetosphere of Uranus.

2. Dispersion relation

A spatially homogeneous anisotropic, collision less magnetoplasma subjected to an external magnetic field $B_0 = B_0\hat{e}_x$ and an electric field $E_{0_x} = (E_0 \sin \nu t\hat{e}_x)$ has been considered. In order to obtain the dispersion relation in this case, the Vlasov-Maxwell equations are linearized. The linearized equations obtained after neglecting the higher order terms and separating the equilibrium and non equilibrium parts, following the techniques of Misra and Pandey [19] are given as

$$\boldsymbol{v}.(\delta f_{s0}/\delta r)+(e_s/m_s)[E_0 \sin \nu t + (\boldsymbol{v}\times B_0/c](\delta f_{s0}/\delta v) = 0, \qquad (1)$$

$E_{0_x} = (E_0 \sin \nu t\hat{e}_x)$

$$(\delta f_{s1} / \delta t) + \boldsymbol{v}.(\delta f_{s1} / \delta r) + (F / m_s)(\delta f_{s1} / \delta \boldsymbol{v}) = S(r,v,t), \tag{2}$$

where force is defined as $F = mdv/dt$,

$$F = e_s [E_0 \sin \nu t + (v \times B_0)/c]. \tag{3}$$

The particle trajectories are obtained by solving the equation of motion defined in eq. (3) and $s(r, \boldsymbol{v}, t)$ is defined as

$$S(r,\boldsymbol{v},t) = (-e_s / m_s)[E_1 + (\boldsymbol{v} \times B_1)/c](\delta f_{s0} / \delta \boldsymbol{v}), \tag{4}$$

where S denotes species and E_1, B_1 and f_{s1} are perturbed quantities and are assumed to have harmonic dependence in f_{s1}, B_1 and $E_1 \equiv \exp i\,(k.\,r\text{-}\omega t)$.

The method of characteristic solution is used to determine the perturbed distribution function.

f_{s1}, which is obtained from eq. (2) by

$$f_{s1}(r,v,t) = \int_0^\infty s\{r_0(r,v,t), \boldsymbol{v}_0(r,\boldsymbol{v},t), t-t'\}\, dt'. \tag{5}$$

The phase space coordinate system has been transformed from (r, v, t) to $(r, \boldsymbol{v}_0, t-t')$ and $t' = t - t'$. The particle trajectories which have been obtained by solving eq. (3) for the given external field configuration and wave propagation

$$\boldsymbol{k} = \left[k_\perp \hat{e}_x, 0, k, \hat{e}_z\right]$$

are

$$X_0 = X + (v_y / \omega_{cs}) + (1/\omega_{cs})\left[v_x \sin\omega_{cs}t' - v_y \cos\omega_{cs}t'\right]$$

$$+ (\Gamma_x / \omega_{cs})\left[(\omega_{cs} \sin \nu t' - v \sin\omega_{cs}t')/(\omega_{cs}^2 - \nu^2)\right],$$

$$Y_0 = Y + (v_x / \omega_{cs}) - (1/\omega_{cs})\left[v_x \cos\omega_{cs}t' - v_y \sin\omega_{cs}t'\right]$$

$$- (\Gamma_x / \nu\omega_{cs})\left[1 + \{(\nu^2 \cos\omega_{cs}t' - \omega_{cs}^2 \cos \nu t')/(\omega_{cs}^2 - \nu^2)\}\right],$$

$$Z_0 = Z - v_z t', \tag{6}$$

and the velocities are

$$\boldsymbol{v}_{x0} = v_x \cos\omega_{cs}t' - v_y \sin\omega_{cs}t' + \left\{\nu\Gamma_x / (\omega_{cs}^2 - \nu^2)\right\}(\cos \nu t' - \cos\omega_{cs}t'),$$

$$\boldsymbol{v}_{y0} = v_y \sin\omega_{cs}t' + v_y \cos\omega_{cs}t' - \left\{\Gamma_x / (\omega_{cs}^2 - \nu^2)\right\}(\omega_{cs} \sin \nu t' - \nu \sin\omega_{cs}t'),$$

$$\boldsymbol{v}_{z0} = v_z, \tag{7}$$

where $\omega_{cs} = (e_s B_0)/m_s$ is the cyclotron frequency of species s

and $\Gamma_x = (e_s E_{0x})/m_s$.

Eq. (4) can be written in terms of perturbed quantities as

$$S(r_0, \boldsymbol{v}_0, t-t') = -(e_s / m_s\omega) e^{i\{kr_0(r,\boldsymbol{v},t)-\omega(t-t')\}} \times [(\omega - k.\boldsymbol{v}_0)E_1$$

$$+(\boldsymbol{v}_0.E_1)\boldsymbol{k}](\delta f_{s0} / \delta \boldsymbol{v}) . \tag{8}$$

After some lengthy algebraic simplification and carrying out the integration, the perturbed distribution function is given as

$$f_{s1}(r,v,t) = (-e_s / m_s\omega) \sum_{m.n.p.q.=-\infty}^{\infty} [(J_p(\lambda_2) J_m(\lambda_1) J_q(\lambda_3) e^{i(k.r-\omega t)}) /$$

$$\{(\omega - k_\parallel v_\parallel - (n+q)\omega_{cs} + pv)\}][E_{1x} J_n J_p \{(n/\lambda_1)U^* + (p/\lambda_2)D_1\}$$

$$-iE_{1y}\{J_n' J_p C_1 + J_n J_p' D_2\} + E_{1z} J_n J_p w^*\}, \tag{9}$$

where the Bessel identity

$$e^{i\lambda/\sin\theta} = \sum_{k=-\infty}^{\infty} J_k(\lambda) e^{ik\theta}$$

has been used, the arguments of the functions are

$$\lambda_1 = (k_\perp v_\perp)/(\omega_{cs})$$

$$\lambda_2 = (k_\perp \Gamma_x \nu)/(\omega_{cs}^2 - \nu^2)$$

$$\lambda_3 = (k_\perp \Gamma_x \nu)/(\omega_{cs}^2 - \nu^2)$$

$$C_1 = (1/v_\perp)(\delta f_0 / \delta v_\perp)(\omega - k_\parallel . v_\parallel) + (\delta f_0 / \delta v_\parallel) k_\parallel,$$

$$U^* = C_1[v_\perp - \{\nu\Gamma_x / (\omega_{cs}^2 - \nu^2)\}],$$

$$w^* = [(n\omega_{cs} v_\parallel / v_\perp)(\delta f_0 / \delta v_\perp) - n\omega_{cs}(\delta f_0 / \delta v_\perp)]$$

$$[1 + \{k_\perp \Gamma_x \nu / (\omega_{cs}^2 - \nu^2)\}\{(p/\lambda_2) - (n/\lambda_1)\}],$$

$$D_1 = C_1\{\nu\Gamma_x / (\omega_{cs}^2 - \nu^2)\}, \quad D_2 = C_1\{\omega_{cs}\Gamma_x / (\omega_{cs}^2 - \nu^2)\},$$

$$J_n' = \{dJ_n(\lambda_1)\}/d\lambda_1 \quad \text{and} \quad J_p' = \{dJ_p(\lambda_2)\}/d\lambda_2 . \tag{10}$$

Following Harris [30] and Misra and Pandey [19], the conductivity tensor $\| \sigma \|$ is written as

$$\|\sigma\| = -\sum (\epsilon_s^2 / m_s\omega) \sum_{m_1 n_1 p_1 q_1 = \infty}^{\infty} \int d^3v [\{J_q(\lambda_3) S_{ij}\} / \{\omega - k_\parallel v_\parallel - (n+q)\omega_{cs} + pv\}], \tag{11}$$

where

$$S_{ij} = \begin{vmatrix} \upsilon_\perp J_n^2 J_p (n/\lambda_1) A & i\upsilon_\perp J_n B & \upsilon_\perp (n/\lambda_1) J_n^2 J_p \dot{W}^* \\ \upsilon_\perp J_n' J_n J_p A & \upsilon_\perp J_n' B & i\upsilon_\perp J_n' J_n J_p W^* \\ \upsilon_\parallel J_n^2 J_p A & i\upsilon_\parallel J_n B & \upsilon_\parallel J_n^2 J_p W^* \end{vmatrix} \tag{12}$$

$$A = \{(n/\lambda_1) U^* + (p/\lambda_2) D_1\},$$

$$B = \{J_n' J_p C_1 + J_n J_n' D_2\}. \tag{13}$$

From $J = \| \sigma \| E_1$ and two Maxwell's curl equations for the perturbed quantities, the wave equation can be obtained as

$$[k^2 - \boldsymbol{k}.\boldsymbol{k} - (\omega^2/c^2) \in (\boldsymbol{k}, \omega)] E_1 = 0, \tag{14}$$

where

$$\| \in (k, \omega) \| = 1 - (4\pi / i\omega) \| \sigma (k, \omega) \| \tag{15}$$

is a dielectric tensor, After using eq. (11), eq. (15) becomes

$$\in_{ij} (k, \omega) = 1 + \sum_s \{(4\pi e_s^2)/(m_s \omega^2)\} \sum_n \sum_p J_p(\lambda_2) J_q(\lambda_3)$$

$$\int (d^3 \upsilon_\parallel S_{ij}) / (\omega - k_\parallel \upsilon_\parallel - (n+q)\omega_{cs} + p\nu)\}. \tag{16}$$

Expression for the growth rate :

The zero order distribution function is written as [14, 19]

$$f_0(\boldsymbol{\upsilon}) = \frac{n_0 \upsilon_\perp^{2j}}{(\pi)^{3/2} \alpha_\perp^{2(j+1)} \alpha_\parallel j!} \exp\left[\frac{\upsilon_\perp^2}{\alpha_\perp^2} - \frac{(\upsilon_\parallel - \upsilon_d)^2}{\alpha_\parallel^2}\right], \tag{17}$$

where j is the distribution index.

When $j = 0$, this reduces to bi-Maxwellian and subsequently for $T_\perp = T_\parallel$ it reduces further to Maxwellian distribution. For $j = 1$, it reduces to loss-cone distribution. The resulting dispersion relation for oblique propagating whistler mode is approximated as

$$\in_{11} + \in_{12} = N^2 \cos^2 \theta_1, \tag{18}$$

on following assumptions $k_\perp = k \sin \theta_1 = 0$ and $k_\parallel = k \cos \theta_1$

where θ_1 is the angle between B_0 and $k_\parallel$.

Hence, the dispersion relation is obtained from this, for order of Bessel function $n = 1$, $p = 1$ and $q = 0$ and putting

$$\sum j_p = 1 \text{ and } \sum j_q = 1$$

$$\frac{k^2c^2\cos^2\theta_1}{\omega^2} = 1+\sum\frac{4\pi e_x^2}{m_s\omega^2}\left\{\frac{2n_0}{\alpha_\perp^{2(j+1)}}j!\right\}\left[x_1\frac{\omega-k_\parallel v_d}{k_\parallel\alpha_\parallel}z(\xi)+x_2\{1+\xi z(\xi)\}\right], \quad (19)$$

where

$$\xi = \frac{\omega-k_\parallel v_d-\omega_c+pv}{k_\parallel\alpha_\parallel},$$

$$x_1 = \frac{\alpha_\perp^{2(j+1)}j!}{2}-\frac{v\Gamma_x}{\omega_c^2-v^2}\frac{\alpha_\perp^{2(j+1)}}{4}(j-\tfrac{1}{2})!, \quad (20)$$

$$x_2 = \frac{\alpha_\perp^{2(j+1)}j!}{2}\left\{\frac{\alpha_\perp^2}{\alpha_\parallel}(j+1)-1\right\}-\frac{v\Gamma_x}{\omega_c^2-v^2}\frac{\alpha_\perp^{2j+1}}{4}\left\{\frac{\alpha_\perp^2}{\alpha_\parallel}(2j+1)-1\right\}(j-\tfrac{1}{2})!.$$

After substituting

$$\frac{k^2c^2\cos^2\theta_1}{\omega^2} >> 1,$$

$$\omega_{ps}^2 = \frac{4\pi e_s^2 n_0}{m_s}, \quad (21)$$

$$\omega = \omega_r + i\gamma,$$

and assuming k to be real and using an asymptotic expansion of $z(\xi)$ in the limit of large value of ξ as

$$z(\xi) = i\sqrt{\pi}\exp(-\xi^2)-\frac{1}{\xi}\left(1+\frac{1}{2\xi^2}\right),$$

$$|\xi| >> 1, \quad \mathrm{Im}|\xi| << \mathrm{Re}|\xi|,$$

the eq. (19) now reduces to

$$D(k,\omega) = \frac{k^2c^2\cos^2\theta_1}{\omega_{ps}^2}+\left\{\frac{1}{\alpha_\perp^{2(j+1)}j!}\right\}\left[x_1\frac{(\omega-k_\parallel v_d)}{k_\parallel\alpha_\parallel}\left\{-\frac{1}{\xi}-\frac{1}{2\xi^3}\right\}\right.$$

$$\left.-x_2\frac{1}{2\xi^2}+\left\{x_1\frac{\omega-k_\parallel v_d}{k_\parallel\alpha_\parallel}+x_2\xi\right\}\left\{i\sqrt{\pi}\exp(-\xi^2)\right\}\right]. \quad (22)$$

The eq. (22) further reduces to simpler numerical dimension-less form. By introduction of the following definitions :

$$k_\parallel = k\cos\theta_1, \quad \bar{k} = \frac{k\alpha_\parallel}{\omega_c},$$

$$x_3 = \frac{\omega_r}{\omega_c}, \qquad x_4 = -\frac{\nu}{\omega_c},$$

$$x_5 = \frac{k_{\parallel} v_d}{\omega_c}, \qquad \beta = -\frac{K_B T_{\parallel} \mu_0 n_0}{B_0^2},$$

$$K_1 = \frac{\alpha_{\perp}^{2(j+1)} j!}{4x_1}, \quad K_2 = x_3 - x_5,$$

$$K_3 = 1 - x_3 + x_4 + x_5,$$

the growth rate and real frequency are in dimensionless form as

$$\frac{\gamma}{\omega_c} = \frac{\dfrac{\sqrt{\pi}}{\bar{k}\cos\theta_1}\left[\left(\dfrac{x_2}{x_1} - \dfrac{K_2}{K_3}\right)K_3^2\right]\exp\left(-\left(\dfrac{K_3}{\bar{k}\cos\theta_1}\right)^2\right)}{1 + x_4 + \dfrac{\bar{k}\cos^2\theta_1(1+x_4)}{2K_3^2} - \dfrac{\bar{k}^2\cos^2\theta_1}{k_3}\left(\dfrac{x_2}{x_1} - \dfrac{K_2}{K_3}\right)} \tag{23}$$

and

$$x_3 = \frac{\omega_r}{\omega_c} = \frac{k^2\cos^2\theta_1}{\beta}\left[K_1(1+x_4) + \frac{x_2}{x_1}\frac{\beta}{2(1+x_4+x_5)}\right] + X_5. \tag{24}$$

3. Plasma parameters

To evaluate quantitatively the real frequency and growth rate for current driven oblique whistler wave, following plasma parameters given by Smith *et al* [8] Bridge *et al* [32] and Ness *et al* [5] suited to the Uranian magnetosphere have been assumed. Density $n_0 = 5 \times 10^4$ m^{-3}, magnetic field intensity $B_0 = 5 \times 10^{-10}$ Tesla. Strength of electric field $E_0 = 4 \times 10^{-3}$ V/m. The effect of electric field frequency variation on the growth rate has been studied for Zero, 3, 6, 9 Hz. Temperature anisotropy $A_T = \left\{\left(\alpha_{\perp}^2/\alpha_{\parallel}^2\right) - 1\right\} = 0.25,\ 0.5,\ 0.75$ where $\alpha_{\parallel}$ and $\alpha_{\perp}$ are the parallel and perpendicular thermal velocities. Various oblique incidence 0, 10 and 20 Degrees and various values of the drift velocities 0, 0.2, 0.6 and 0.8 have been taken for evaluation of growth rate.

4. Results and discussion

Figure 1 describes variation of the normalized growth rate and real frequency with normalized wave number at various anisotropies for bi-Maxwellian plasma, $j = 0$ and for other fixed parameters. It is obvious that the increase of anisotropy increases the growth rate but the Maxima significantly shifts towards lower $\bar{k}$ [frequency value], at the same time the band width also reduces significantly. For all the given values of the temperature anisotropies, there is sharp rise in the growth rate for its maxima at a particular value of $\bar{k}$. This shows that the temperature anisotropy remains the prime source of seeding the free energy to the plasma.

Figure 2 shows the variation of the growth rate with normalized wave number for various values of the drift velocity of electrons parallel to the magnetic field at other fixed parameters. The growth rate changes significantly with the increase of the drift velocity. The character of

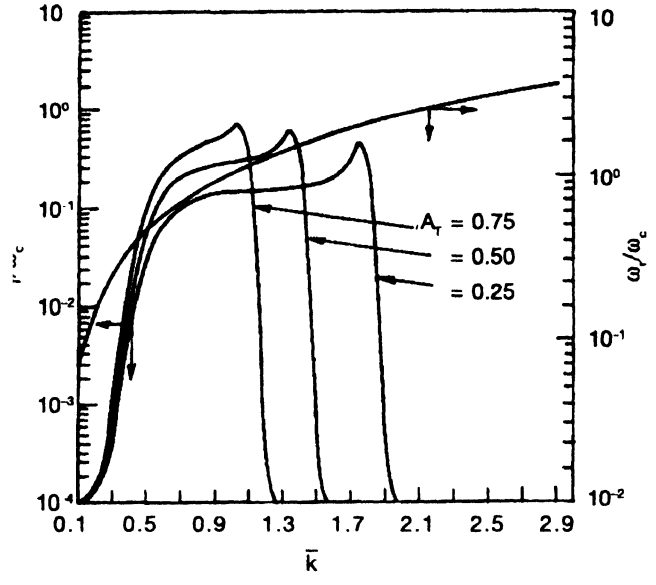

Figure 1 : Variation of normalized growth rate (γ/ω_c) and real frequency (ω_r/ω_c) with normalized wave number $\bar{k}$ at various anisotropies for bi-Maxwellian plasma, $j = 0$ at other fixed plasma parameters, $E_0 = 4 \times 10^{-3}$ V/m, $\nu = 9$Hz, $\theta_1 = 20^0$, $\nu_d = .8$, $n_0 = 5 \times 10^4$ m^{-3}, $B_0 = 5 \times 10^{-10}$ T

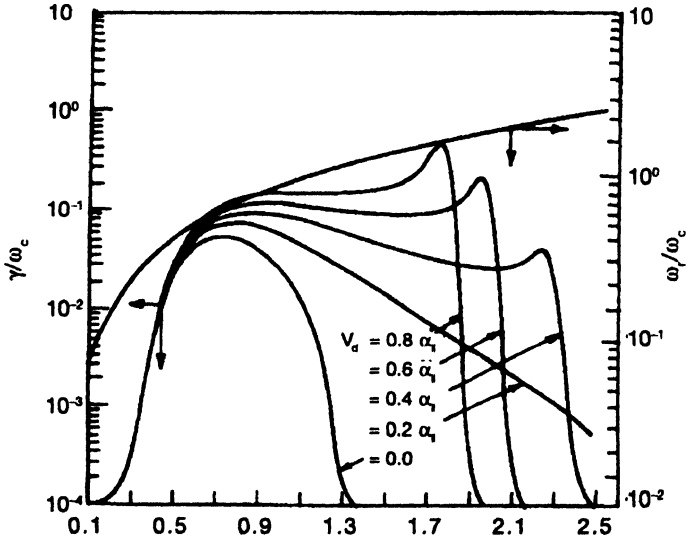

Figure 2 : Variation of normalized growth rate (γ/ω_c) and real frequency (ω_r/ω_c) with normalized wave number $\bar{k}$ at various drift velocities for bi-Maxwellian plasma, $j = 0$ at other fixed plasma parameters, $E_0 = 4 \times 10^{-3}$ V/m, $\nu = 9$Hz, $\theta_1 = 20^0$, $n_0 = 5 \times 10^4$ m^{-3}, $B_0 = 5 \times 10^{-10}$ T, $A_T = .25$.

current driven oblique whistler differs depending upon the value of v_d. In the absence of the drift velocity the curve shows a maxima on the lower side of $\bar{k}$ value, a slight increase of the drift velocity increases the growth rate and the band width. But further increase of the value of the drift velocity shows double peaks in the growth rate curve one on the lower and the other on the higher side of the $\bar{k}$ values. Although the further increase of the drift velocity increases the growth rate maxima on both the sides but the band width goes on reducing. Simultaneous presence of double peaks for higher values of drift velocity suggests modification of usual real frequency in generation of a new wave. Here either electrostatic modes are generated or polarization is getting reversed. In between the peaks growth reduces but never goes to zero. In this case it remains in left hand polarized mode. The results are in agreement with satellite observations and results reported by Smith *et al* [8] and Wong and Smith [25].

Figure 3 represents the effect of a.c. frequency variation on the growth rate for a bi-Maxwallian plasma $J = 0$. As the frequency increases, the growth rate increases with a decrease in the band width and shift of maxima towards lower $\bar{k}$ values, thus covering a wide spectrum of frequencies. In this case also, there is double peak in the growth rate and the generated frequencies obtained are in agreement with Smith *et al* [8] and Wong and Smith [25]. While the beam of bi-Maxwellian plasma generated simultaneously two peaks at different frequencies

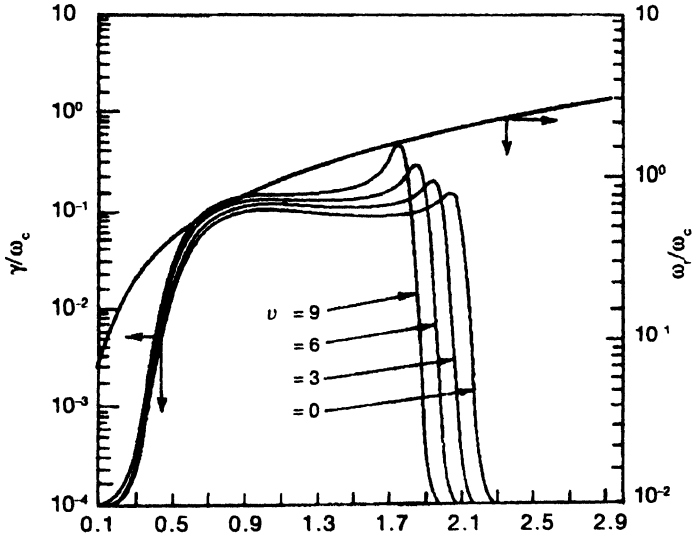

Figure 3 : Variation of normalized growth rate (γ/ω_c) and real frequency (ω_r/ω_c) with normalized wave number $\bar{k}$ for various values of a.c. frequency for bi-Maxwellian plasma, $j = 0$ at other fixed plasma parameters, $E_0 = 4 \times 10^{-3}$ V/m, $\theta_1 = 20^0$, $n_0 = 5 \times 10^4$ m^{-3}, $B_0 = 5 \times 10^{-10}$ T, $v_d = .8$ $A_T = .25$.

with the growth rate not tending to zero in between two maximas, but as shown in Figure 4 the energetic loss-cone beam generated only one peak in the growth rate curve and alters the range of generated whistler frequencies. Although there is no change in the growth rate with the increase of a.c. frequency but like bi-Maxwellian plasma the increase in the a.c. frequency decreases the band width, a result in conformity with satellite observations and reported low frequency whistler wave emissions interpreted as lower hybrid emissions excited by the

electrostatic ion loss-cone instability [33]. The loss conebeam is more effective than bi-Maxwellian beam.

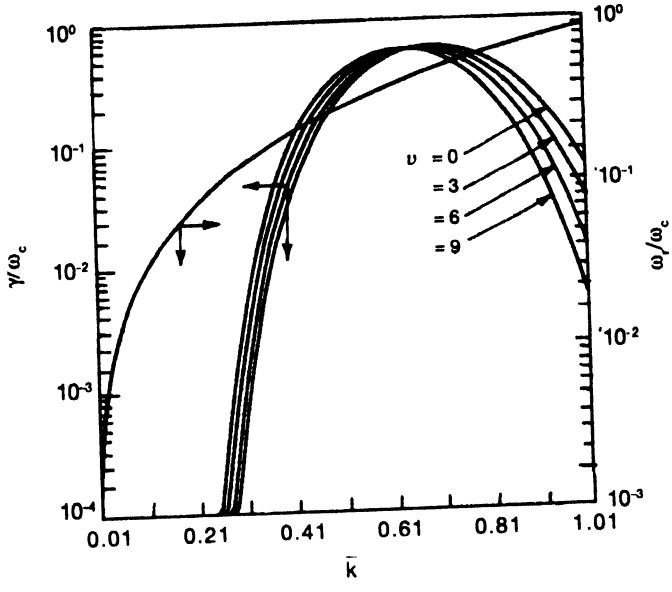

Figure 4 · Variation of normalized growth rate (γ/ω_c) and real frequency (ω_r/ω_c) with normalized wave number $\bar{k}$ at various values of a.c frequency for loss-cone plasma, $j = 1$ at other fixed plasma parameters, $E_0 = 4 \times 10^{-3}$ V/m, $\theta_1 = 20^0$, $n_0 = 5 \times 10^4$ m^{-3}, $B_0 = 5 \times 10^{-10}$ T, $v_d = .8$, $A_T = .25$

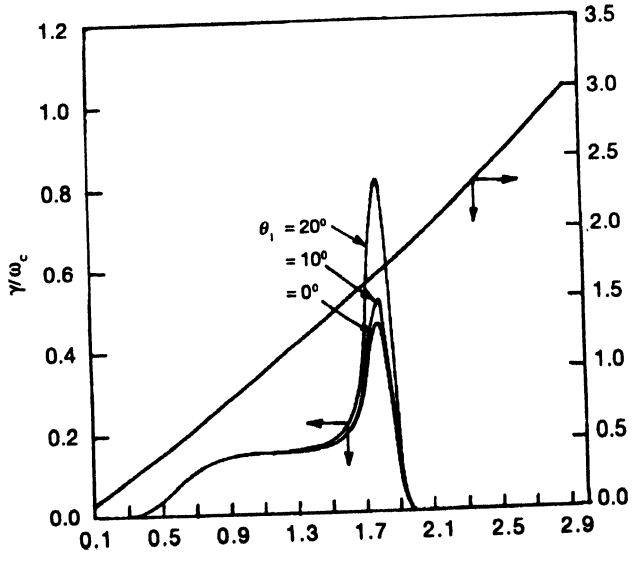

Figure 5 : Variation of normalized growth rate (γ/ω_c) and real frequency (ω_r/ω_c) with normalized wave number $\bar{k}$ at various values of angle of propagation θ_1, for bi-Maxwellian plasma $j = 0$ at other fixed plasma parameters, $E_0 = 4 \times 10^{-3}$ V/m, $\nu = 9$Hz, $n_0 = 5 \times 10^4$ m^{-3}, $B_0 = 5 \times 10^{-10}$ T, $v_d = .8$, $A_T = .25$.

Figure 5 gives the variation of growth rate for various $\bar{k}$ values of angle of propagation θ_1, at other fixed plasma parameters. In this case also the growth rate shows double peak. Growth rate from $0^\circ - 20^\circ$ has significant effect on other peak on the higher side of $\bar{k}$ values. The second peak shows sharp rise in the growth rate curve with the change in the angle of propagation, having rapid fall off to both higher and lower frequencies indicating that the secondary peak of whistler emission in quite narrow banded, thus showing a possibility of simultaneous generation of two-whistler waves at different frequencies.

From all figures, it is clear that our results are very much in the order of the observed normalized frequency range of whistler emissions at Uranus as reported by Coroniti *et al* [4].

Acknowledgment

The authors are grateful to Dr. K. D. Misra, Professor of Applied Physics, I.T. (B.H.U.) for providing laboratory facilities.

References

[1] D A Gurnett, W S Kurth, F L Scraf and R L Poynter *Sci.* **233** 106 (1986)

[2] W S Kurth, D A Gurnett and F L Scarf *J. Geophys Res.* **91** 11958 (1986)

[3] F L Scarf, D A Gurnett, W S Kurth and R L Poynter *Adv. Space Res.* (in Press) (1986)

[4] F V Coroniti, W S Kurth, F L Scarf, S M Krimigis, C F Kennel and D A Gurnett *J. Geophys. Res.* **92** 15234 (1987)

[5] N F Ness, M H Acuna, K W Behannon, L F Burlaga, L E P Connerney, R P Lepping and F M Neubauer *Sci.* **233** 85 (1986)

[6] D S Orlowski, C T Russsell and R P Lepping *J Geophys Res.* **97** 19187 (1992)

[7] C W Smith, M L Goldstein and H K Wong *J. Geophys. Res.* **94** 17035 (1989)

[8] C W Smith, H K Wong and M L Go *J. Geophys. Res.* **96** 15841 (1991)

[9] F S Mozer, R B Torbert, U V Fahleson, C G Fathauer, A Gonfalone, AaPedersen and C T Russel *Space Sci. Rev* **22** 791 (1978)

[10] J R Wygant, M Bensadoun and F S Mozer *J. Geophys Res.* **92** 109 (1987)

[11] P A LindGuist and F S Moger *J. Geophys Res* **95** 137 (1990)

[12] J La Belle and R A Treumann *Space Sci. Rev* **47** 175 (1988)

[13] C J Farrugia, R P Rijnbeck, M A Saunders, D J Southwood, D J Rodgers, M F Smith, D S Hall, P J Christiansen and L J C Williscroff *J. Geophys. Res.* **93** 14465 (1988)

[14] S Sazhin *Planet Space Sci* **36** 1111 (1988)

[15] S Sazhin *Whistler Mode Waves in a Hot Plasma* (*Cambridge Atmospheric and Space Science Series*) (Cambridge Univ. Press, New York) (1993)

[16] B T Tsurutani, E J Smith, R M Thone, R R Anderson, D A Gurnett, G K Parks, C S Lin, C T Russel *Geophys. Res Lett.* **8** 183 (1981)

[17] B T Tsurutani, A L Brinca, E J Smith, R T Okida, R R Anderson, T E Eastman *J Geophys. Res.* **79** 118 (1989)

[18] K D Misra and T Haile *J. Geophys. Res* **98** 9297 (1993)

[19] K D Misra and R S Pandey *J Geophys Res.* **100** 19405 (1995)

[20] A Korth, G Kremser, S Peraut and A Roux *Planet Space. Sci.* **32** 1393 (1984)

[21] A K Ward, D A Bryant, T Edwards, D J Parker, A Ohea, T J Patrick, P H Sheather, K P Barnstada, A M Cruise *The AMPTE-UKS spacecraft IEEE Transactions on Geoscience and Remote sensing* **GE-23** 202 (1985)

[22] C F Kennel F V Coroniti and F L Scraf *J. Geophys. Res.* **91** 1424 (1986)

[23] Y L Zhang, H Matsumoto and Y Omura *J. Geophys. Res.* **98** 21353 (1993)

[24] P E Devine, S C Chapman and J W Eastwood *J. Geophys. Res.* **100** 17189 (1995)

[25] H K Wong and C W Smith *J. Geophys. Res.* **99** 13373 (1994)

[26] L H Lyu and J H Kan *Geophys. Res. Lett.* **17** 1041 (1990)

[27] F G Pantellini, E A Heron, J C Adam and A Mangenery *J. Geophys. Res.* **97** 1303 (1992)

[28] V A Thomas, D Winske and N Omidi *J. Geophys. Res.* **95** 18809 (1990)

[29] D Winske, N Omidi, K B Quest and V A Thomas *J. Geophys. Res.* **95** 18821 (1990)

[30] L Borda de Agua, Y Omura and H Matsumoto *J. Geophys. Res.* **101** 15475 (1996)

[31] E G Harris **158**, in *Physics of Hot Plasmas*, eds. by R Oliver and T Boyd (Edinburgh) (1970)

[32] H S Bridge *et al Science* **232** 89 (1986)

[33] F V Coroniti, R W Fredricks and R White *J. Geophys. Res.* **77** 6243 (1972)